Oceanic responses to gradual transitions of equator-to-pole temperature-gradients

By W. CAI[1]* and P. C. CHU[2]

[1]*CSIRO Division of Atmospheric Research, Australia*
[2]*Naval Postgraduate School, Monterey, USA*

SUMMARY

Responses of an ocean model to gradual transitions of equator-to-pole gradients show that several quasi-equilibrium states within the thermally driven regime are generated under identical forcing conditions. These different states are associated with different patterns (the location and the penetration depth) of oceanic convection. Small changes in the thermal forcing conditions can push the system into an oscillatory regime. Once in this regime, oscillations appear to proceed as internal processes. One important implication of these results is that the present-day ocean climate may not recover fully if the atmospheric CO_2 level, after doubling, is lowered to the present-day level.

KEYWORDS: Thermohaline circulation   Climate changes   Multiple equilibrium   Interdecadal oscillations   Thermohaline

1. INTRODUCTION

A common feature of the response of an atmosphere–ocean coupled model to transient CO_2 increase is an interhemispheric asymmetry in surface warming, with a slower warming in the southern hemisphere than in the northern hemisphere (Stouffer *et al.* 1989; Manabe *et al.* 1990, 1991; Cubasch *et al.* 1992; Murphy and Mitchell 1995). The processes for generating this feature have been investigated extensively in many studies (e.g., Bryan *et al.* 1988; Stouffer *et al.* 1989; Manabe *et al.* 1990, 1991). In the northern hemisphere, there is a poleward amplification of the increase in surface temperature. The initial warming associated with the CO_2 increase causes a poleward retreat of sea ice and snow cover in the northern hemisphere. These lead to a decrease in surface albedo, the amplitude of which increases poleward. Such a poleward amplification is absent in the southern hemisphere. Manabe *et al.* (1991) further showed that the asymmetric response also occurs in response to a transient CO_2 decrease, with a faster cooling and a poleward amplification of cooling in the northern hemisphere. A poleward amplification of warming (cooling) means that the equator-to-pole temperature-contrast of the present-day climate is reduced (enhanced). A question arises as to whether the climate would recover its present state if the CO_2 level, after doubling, were to return to its present level. The ultimate answer to the question needs to be obtained through a realistic coupled model. However, given the importance of the thermohaline circulation in determining the response of a coupled system to a CO_2 increase (Manabe and Stouffer 1993, 1994), some insights may be gained from results of an ocean-only model. In the context of a somewhat mechanistic study, the present paper investigates the quasi-equilibrium response of the thermohaline circulation in an ocean-alone model to an imposed decrease in the equator-to-pole temperature-gradient. The response is compared with that to an imposed increase of a temperature gradient of *identical* magnitude.

* Corresponding author: CSIRO, Division of Atmospheric Research, PMB1 Aspendale, Victoria 3195, Australia.

The behaviour of the present-day thermohaline-circulation has been studied extensively following the pioneering work of Stommel (1961). He showed with a one-hemisphere, simple box model, that the thermohaline circulation has two different modes: one thermally driven that has deep-water formation in the polar region, and one salt driven that has deep-water formation near the equator. In a two-hemisphere, simple general circulation model, Bryan (1986) showed that the transition may occur between a northern hemispheric high-latitude sinking cell and a southern hemispheric one. The northern and southern high-latitude sinking cells would correspond to the North Atlantic Deep-Water Formation (NADWF) and the Antarctic Bottom Water formation cell in a more realistic model. Ocean-only model studies suggest that the flip between a NADWF-on mode and a NADWF-off mode can be induced easily (Weaver and Sarachik 1991a,b). Observations of deep-sea cores indicated that there are modes which have less extreme outcomes than one with NADWF on the one hand and one in which NADWF completely disappears on the other (Oppo and Fairbanks 1990). (A transition between these modes can, however, be rather rapid.) Further, it is likely that there is a continuum of circulation modes (Raymo *et al.* 1990). This appears to be supported by results from highly simplified coupled models (Stocker and Wright 1991; Rahmstorf 1995a). In these models, fresh-water forcing at high latitudes is gradually increased and then gradually decreased to the original magnitude. A spectrum of modes is found, and, when a threshold value is exceeded, a sudden transition takes place from a mode with NADWF to one without. It was further shown that multiple convection-patterns may occur under identical surface-forcings, and transitions between convection patterns may be induced by a step-function forcing, gradual forcing, or stochastic forcing over large areas or at single grid-points (Lenderink and Haarsma 1994, 1996; Rahmstorf 1995a,b; Weaver and Hughes 1994).

Manabe and Stouffer (1988) gave the first example of the two stable modes in a coupled ocean–atmosphere model. Maier-Reimer and Mikolajewicz (1989) applied this idea of multiplicity to the Younger Dryas period as an explanation. However, Duplessy *et al.* (1988) and Bond et al. (1993) pointed out that, although NADWF was reduced and shifted southward during the glacial period, it was neither shut off, nor replaced by a salt-dominated sinking at the equator. Coupled-model experiments (Manabe and Stouffer 1995; Cai *et al.* 1997) indicated that the thermohaline circulation is quite stable at present and that an extremely large perturbation would be needed to bring about a transition from the present thermally driven regime to a salt-driven regime. Huang et al. (1992) extended the work of Stommel (1961). They found that besides the two major modes of the Stommel (1961) model, the thermohaline circulation can have many solutions under an identical set of surface forcings, and that some of these solutions are only slightly different. A question arises as to whether the thermohaline circulation exhibits similar behaviour in response to changes in atmospheric thermal conditions. This is one of the central issues of the present paper.

We investigate the quasi-equilibrium response of a model NADWF to a change in atmospheric thermal conditions. In terms of parameter range, it is within a thermally driven regime, rather than varying from a thermally driven to a salt-driven one. Hence this serves as a supplement for a more complete understanding of the NADWF circulation. We show that within the thermally driven regime, responses of the thermohaline circulation to anti-symmetric changes in atmospheric thermal conditions are not antisymmetric with respect to time. Many different quasi-equilibrium states may exist under identical atmospheric conditions. Changes in the atmospheric thermal-forcing condition can push the thermohaline circulation into a thermal oscillatory regime. We demonstrate that upon the removal of the change in the atmospheric thermal condition, thermohaline circulation does not fully return to the state existing before the change of forcing.

TABLE 1. DISTRIBUTION OF VERTICAL LEVELS

Level	Thickness (m)	Depth of (T, S) (m)
1	25	12.5
2	25	37.5
3	40	70
4	70	125
5	110	215
6	200	370
7	330	635
8	450	1025
9	650	1575
10	900	2350
11	900	3250
12	900	4150

TABLE 2. VALUES OF MODEL COEFFICIENTS

Parameter	Symbol	Value
Horizontal diffusivity	A_{TH}	$1 \times 10^3 \ \mathrm{m^2 s^{-1}}$
Horizontal viscosity	A_{MH}	$3 \times 10^5 \ \mathrm{m^2 s^{-1}}$
Vertical diffusivity	A_{TV}	$1 \times 10^{-4} \ \mathrm{m^2 s^{-1}}$
Vertical viscosity	A_{MV}	$1 \times 10^{-4} \ \mathrm{m^2 s^{-1}}$

2. THE MODEL AND FORCING CONDITIONS

The study reported in the present paper employs the Pacanowski et al. (1991) version of the Bryan–Cox–Semtner ocean general circulation model, which is based on the work of Bryan (1969). The model has a width of 60° and a length of 144° extending from 72°S to 72°N. The model southern hemisphere includes a Drake Passage from 44°S to 60°S and a sill 2350 m deep in the Passage; elsewhere the model southern hemisphere is flat-bottomed. The horizontal grid-spacing is 4° of latitude by 4° of longitude. The model has 12 levels at depths listed in Table 1. The various model coefficients are listed in Table 2.

Initially, the model is spun up to a steady state by restoring the model surface-temperature and salinity profiles to those used by Cai (1996b) (his Fig. 1), which approximate the zonal-mean observational annual-mean values. No seasonal forcing is included. The restoring time is 60 days for salinity and 30 days for temperature. We choose a longer timescale for salinity to produce a fresh-water flux with more realistic magnitudes (Tziperman et al. 1994; Cai 1996a). The zonal wind stress used by Bryan (1987) is applied. Only during the first 11 000 years (88 000 years at bottom level) of the spin-up is the technique of Bryan (1984) used. By then, the spin-up reaches a statistically steady state. Then the integration is extended for another 1000 years without the acceleration for a final steady state. From the steady state, a fresh-water flux FS_{spin} and a heat flux FH_{spin} are diagnosed. Thereafter, the forcing condition for salinity is switched from the restoration to the diagnosed flux-condition, and the thermal-forcing condition is switched to the new form we shall describe below. Given a restoring temperature T_0 and a spin-up steady- state sea surface temperature (SST) field T_s, the FH_{spin} satisfies
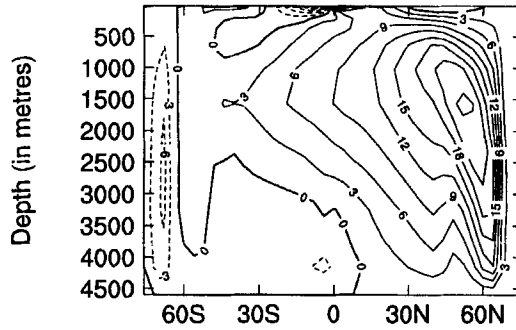
$$FH_{spin} = K_H(T_0 - T_s). \tag{1}$$

Figure 1.   Overturning streamfunction (Sverdrup) from the control run. See text for details of the run.

Here, K_H is the damping rate during the spin-up. The thermal forcing is then switched to

$$Q_{ao} = (1 - \gamma) F H_{spin} + \gamma K_H (T_a - T_1), \; (\gamma < 1) \tag{2}$$

to achieve a weaker damping. In (2), γK_H is the new damping rate, and T_1 is the time-dependent temperature of the uppermost level. At the moment of switching, only the damping rate changes; the heat flux remains exactly the same as before the switch. Subsequently, the heat flux is allowed to change. In this study, we use a value of $\gamma = 0.25$ so that γK_H gives an equivalent thermal-damping timescale of 120 days. With a thickness for the uppermost level of 25 m, this is equivalent to about 9.8 W $m^{-2}K^{-1}$. Such a timescale is close to that adopted by Marotzke (1994), on which his model produced a realistic basin-mean SST-contrast between the Atlantic and the Pacific. This can be justified as a basin-mean version of the simple atmospheric model of Rahmstorf and Willebrand (1995) with an intermediate thermal damping strength. In an extreme case (when γ is chosen to be small so that γK_H is equivalent to 2–3 W $m^{-2}K^{-1}$, i.e., a radiative damping strength), the thermal boundary condition expressed by (2) is equivalent to a simple coupling between a Schopf's (1983) thermal atmospheric model and a mixed-layer ocean (see Cai and Chu (1996) for details).

The model under the thermal forcing of (2) and under the diagnosed FS_{spin} is run to a new steady state, hereafter referred to as the steady state of the control run. There is no oscillation in this steady state. The overturning circulation is shown in Fig. 1. It is qualitatively similar to that in the real world Atlantic. It features a northern sinking cell similar to (and hereafter referred to as) the NADWF cell, and an Antarctic Circumpolar Convective cell.

Subsequently, we perturb the steady state of the control run by adding a time-dependent change to the T_a in the northern hemisphere, so that the new restoring temperature T_A

$$T_A = T_a + \alpha(t)\Delta T(\phi).$$

Here $\alpha(t)$ is a function of model time t; $\Delta T(\phi)$ is a linear function of latitude ϕ, and has the value zero at the equator and a maximum of 2.5°C at northernmost grid points. It is noted that in CO_2 experiments using coupled atmosphere–ocean models, the presence of sea ice causes SSTs not to increase much in polar latitudes. Indeed, in the southern polar region, SSTs even decrease with increasing latitude (Manabe et al. 1991; Gordon and O'Farrell 1997; Cai and Gordon 1998). In the northern hemisphere, SSTs increase with latitude from the equator to about 65°N, where there is a maximum, then decrease towards the poles. Because there is no sea-ice dynamics in the present model, the decrease
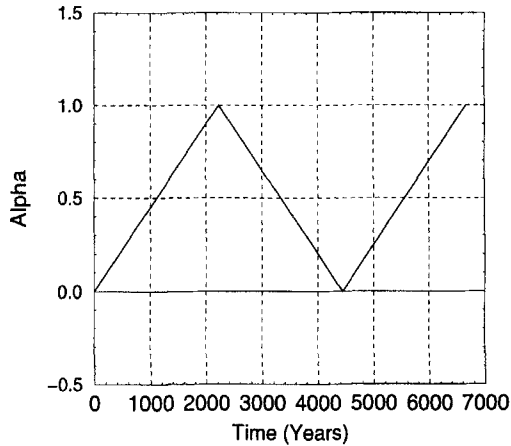
Figure 2. Evolution of $\alpha(t)$. During Stage 1, $\alpha(t)$ is increased from 0 to 1 in a time-span of 2225 years; during Stage 2, $\alpha(t)$ is decreased from 1 to 0 in an identical time-span; In Stage 3, $\alpha(t)$ increases again, as in Stage 1.

from the maximum to the poles is not considered here. The evolution of $\alpha(t)$ is shown in Fig. 2. In Stage 1, in a time-span of 2225 years, $\alpha(t)$ increases from zero to one, so that the equator-to-pole temperature-gradient is decreased linearly. In Stage 2, the model integration continues from the end state of Stage 1. Within an identical time-span $\alpha(t)$ decreases linearly from 1 to 0, restoring the equator-to-pole temperature-gradient to that existing before the Stage 1 integration. In Stage 3, $\alpha(t)$ is increased again as in Stage 1. As will become clear later, the chosen time-span is long enough to allow a quasi-equilibrium behaviour.

3. MODEL RESULTS

Figure 3(a,b,c) shows the maximum overturning of the northern sinking cell as a function of time at Stages 1, 2, and 3. Figure 3(d) shows the evolution as a function of $\alpha(t)$. During Stage 1, as the equator-to-pole contrast of the restoring temperature decreases, the overturning declines. From year 680 to year 750 (Fig. 3(a)), when $\alpha(t)$ increases by about 0.31 to 0.35 (corresponding to a decrease in the equator-to-pole T_A-contrast from about 0.75 degC to about 0.8 degC), the maximum overturning undergoes a sudden increase of about 3 Sv. In order to check whether or not the sudden jump occurs because the initial state is not completely steady, the control run is continued for another 11 000 years. No appreciable change is seen, confirming that the rapid change is a response to the change in the equator-to-pole restoring temperature-gradient. Examination reveals that such a rapid increase is associated with changes in convection penetration depths and locations (the pattern of convection). Before the jump, the depth of maximum overturning deepens and moves to a higher latitude, and convective activities become increasingly concentrated on the north-eastern corner. As the equator-to-pole T_A-contrast decreases further, the strength of convection weakens. During Stage 2, the equator-to-pole T_A-gradient is gradually returned to that which existed before to Stage I. The maximum overturning increases. The two curves of the evolution of the maximum overturning for Stage 1 and Stage 2 do not coincide. Further, during Stage 2, oscillations take place on a timescale of 23 years. We have carried out two experiments with fixed $\alpha(t)$ halfway through Stages 1 and 2. Each experiment is run to a new steady state. The solution of the new steady state differs only slightly from the corresponding quasi-equilibrium state, indicating that the time-span is
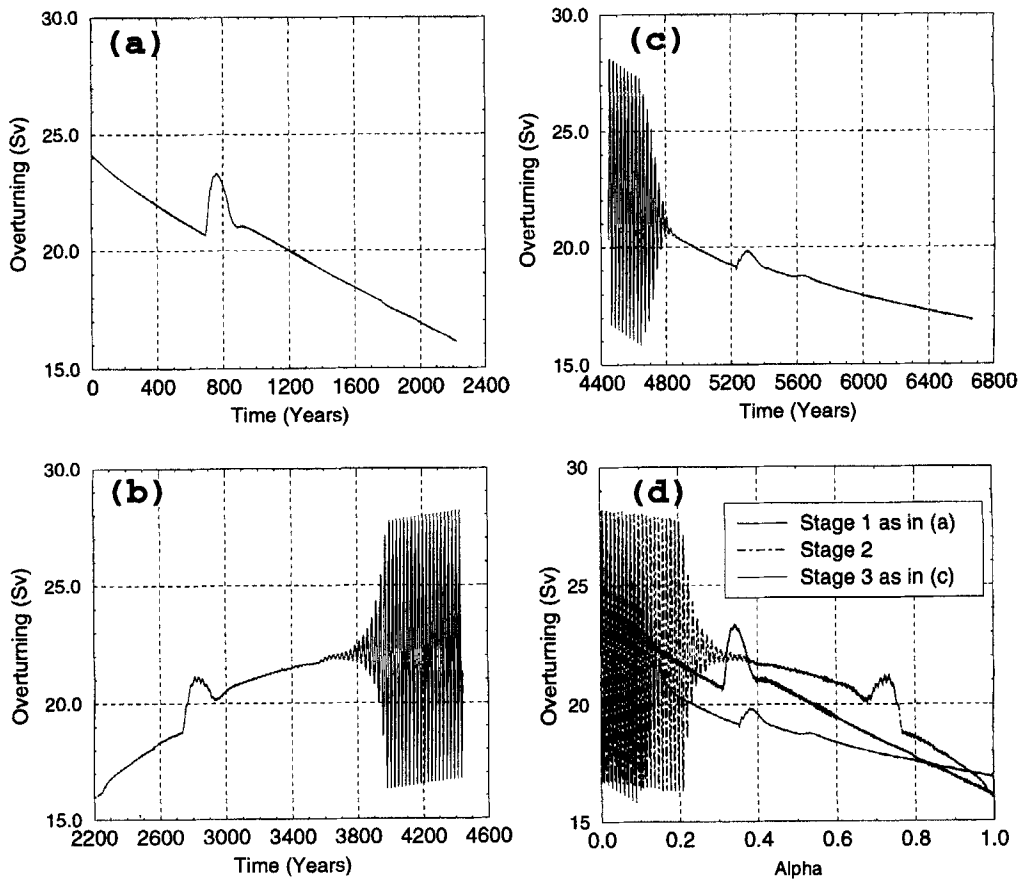
Figure 3. Evolution of the maximum northern overturning (Sverdrup) as a function of time: (a) Stage 1; (b) Stage 2; (c) Stage 3. Panel (d) shows the evolution as a function of the equator-to-pole contrast of the restoring temperature, expressed via $\alpha(t)$ (see text).

long enough to allow a quasi-equilibrium response. Thus, for a given $\alpha(t)$, there are several quasi-equilibrium states. In Stage 3, the equator-to-pole T_A-gradient is decreased again, but the evolution of the model NADWF takes a different path from those of Stages 1 and 2. When the equator-to-pole T_A-contrast is varied backwards and forwards, the evolution of the model maximum NADWF does not coincide with the path of the previous Stages of integration.

These different states of quasi-equilibrium are associated with the nonlinearity of the system. Although changes in T_A are antisymmetric with respect to time, the vertical distribution of temperature (and salinity) is not, neither is the static stability of water columns. During Stage 1, as the equator-to-pole T_A-contrast reduces, the static stability progressively increases except in the north-eastern corner where, from year 680 to year 750, convective activities increase. By halfway through Stage 1, the convective mixed-layer thickness is reduced. During Stage 2, the equator-to-pole T_A-contrast increases, convective activities intensify, and the convective mixed layer deepens. Figure 4(a,b) shows the convection patterns at years 1112.5 (State I) and 3337.5 (State II). Both are at a time when the value of $\alpha(t)$ is 0.5, and the model is under identical forcing conditions. We see that, in State II, the convection in the north-eastern corner, and at the northernmost grid-
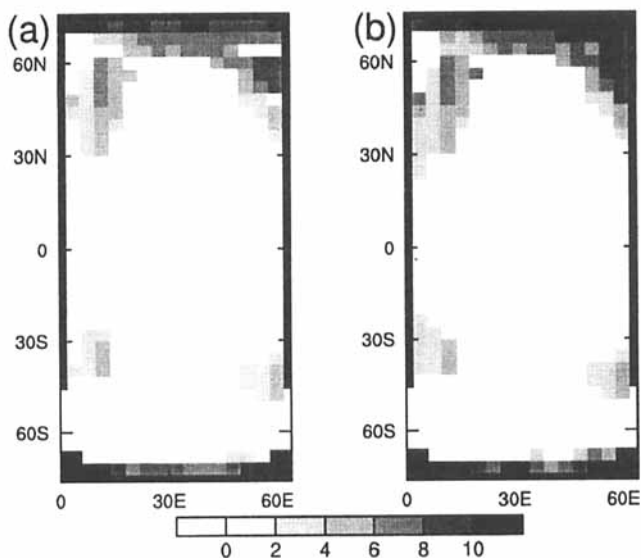
Figure 4. Model levels to which convective penetration reaches: (a) at year 1112.5 (State I); (b) at year 3337.5 (State II). Both are at a time when $\alpha(t) = 0.5$.

points, is stronger than that in State I. Associated with this difference is a stronger poleward heat-transport in State II, a state with a weaker stratification of water column, and raised SSTs. These differences in vertical structure ensure that the response of the thermohaline circulation to a subsequent change in the thermal forcing is considerably different. Manabe *et al.* (1991) found that the responses of a coupled system to two transient antisymmetric CO_2 forcings are generally opposite in sign but not antisymmetric. They showed that the penetration depths of the positive and negative anomalies were quite different, with the anomalies in the increasing CO_2 case being much shallower. In their study, Manabe *et al.* (1991) found further support for these features in experiments using an identical atmospheric model coupled to a mixed-layer ocean. Their results are thus in line with those of the present study. In other ocean model studies (e.g., Stocker and Wright 1991; Rahmstorf 1995a,b), when the fresh-water flux at North Atlantic high latitudes is gradually increased and then gradually decreased to the original magnitude, many solutions were generated for an identical set of surface forcings. Here, it is interesting that a small change in the thermal forcing condition can also generate convective instability. The result highlights the point that, once the pattern of convection is shifted, it is not easily restored (Rahmstorf 1995a), no matter whether it is thermal or haline forcing which drives the shift.

Figure 3(b) covers a period in which oscillations develop. We see that they quickly become regular. An important question regarding the interdecadal variability is whether it is an internal process or one which is excited externally. Internal variability in ocean-only models under a constant flux-forcing (e.g., Huang and Chou 1994; Cai *et al.* 1995) suggested the former was the case. However, Griffies and Tziperman (1995) suggested that oceanic variability could be driven by changes in atmospheric forcing. The results from the present study appear to reconcile the two possibilities. We see that changes in the atmospheric thermal condition can push the system to an oscillatory regime. This is clear from the extended control run (integrated for a further 11 000 years), in which no oscillation was generated. On the other hand, once it is in an oscillatory regime, within a certain range of atmospheric forcing conditions, the oscillation is hardly affected by the
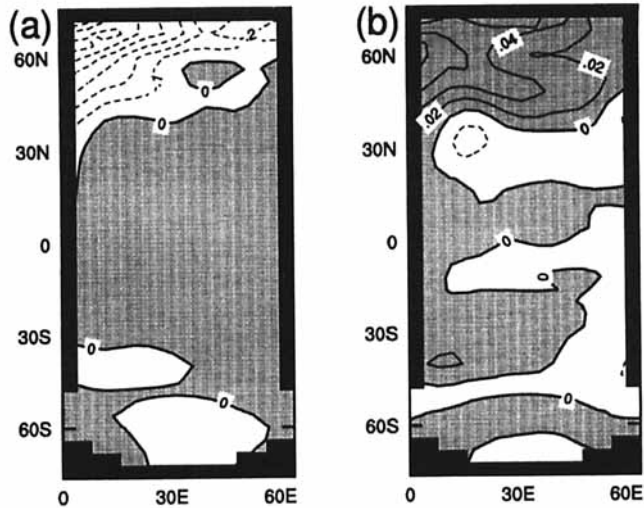
Figure 5.   Surface density anomaly (kg m^{-3}) from a time average over ten oscillation cycles: (a) associated with surface-temperature anomaly; (b) associated with surface-salinity anomaly.

forcing, and the oscillation proceeds as an internal process. Rahmstorf (1995a) found a similar reconciliation. In his study, changes in fresh-water flux-forcing put their system into an oscillatory regime. This similarity is not surprising because it is the change in buoyancy flux that is important.

A detailed examination reveals that the oscillation found during the present study is associated with boundary waves that propagate along the model basin (Winton 1996; Greatbatch and Peterson 1996; Cai and Chu 1998). During Stage 2, as the equator-to-pole T_A-contrast intensifies, the stratification of water columns gradually decreases, the maximum overturning gradually increases and moves polewards, and convective activities concentrate in the north-eastern corner. This causes the northern boundary to be occupied by warm anomalies. As the positive SST anomalies develop in the east, the east–west pressure-gradient increases, further enhancing the northward flow. The anomalous flow then causes the warm anomaly to propagate westwards. The weak or non-existent stratification along the northern boundary impedes the movement along the leading edge, leading to the interdecadal timescale. The large heat-increase in the north-western corner then causes a decrease in the east–west pressure-gradient. As a result, the overturning decreases to a minimum, and cold anomalies develop at the north-eastern corner and propagate westwards, in association with the opposite phase of the oscillation. The wave in the present study is a westward-propagating Rossby wave rather than the Kelvin wave suggested by Winton (1996) and Greatbatch and Peterson (1996). Cai and Chu (1998) discussed the detailed mechanism. In particular, they showed that, once β-effects are removed, no oscillations are generated. It is not clear how the oscillation is affected when model topography is included, which has been found to dampen oscillations in idealized ocean models (Winton 1997).

Figure 5(a,b) shows the surface density-anomaly associated with surface-temperature and surface-salinity anomalies respectively. These anomalies are averages over 10 oscillatory cycles. Those associated with temperature anomalies are the stronger, which suggests that the oscillation is thermally driven, even though it is the change of the surface buoyancy-flux that is important. When these experiments are repeated using identical conditions, except for using a restoring timescale which is the same as in the spin-up (that is,
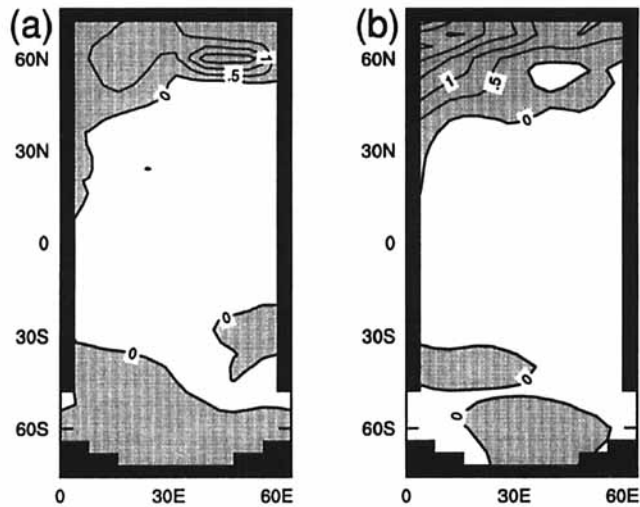
Figure 6. Sea surface temperature differences: (a) between the state at year 1112.5 (State I) and that at year 3337.5 (State II) (both when $\alpha(t) = 0.5$); (b) between the warm and cold phases of a typical oscillation.

$\gamma = 1$ in (1)), the behaviour of the thermohaline circulation is reproduced but no oscillation is generated. In experiments using γ smaller than 0.25, similar oscillations are generated. During Stage 3, the maximum overturning decreases (Fig. 3(c)) and moves equatorwards. The oscillations continue for another 300 years, showing the strong inertia of the system. Thereafter, the amplitude of oscillation decreases rapidly, for the following reasons. Firstly, because of the southward shift of the maximum overturning, less and less heat is pumped into the north-eastern corner. Secondly, because of the weakened convective activities, the stratification of water columns along the northern boundary increases greatly, and so increases the propagation speed of any remaining anomalies.

Although the difference between states within the thermally driven regime may be regarded as small, the consequences for climate can be significant. Figure 6(a) shows SST difference between States II and I, and Fig. 6(b) shows it between the warm and cold phases of a typical oscillation: the SST difference associated with the two quasi-equilibrium states reaches 1.5 degC, and the difference between the two phases reaches 2.5 degC. Changes also take place in the southern hemisphere. For example, the modelled Antarctic Circumpolar Current changes from 108 Sv in State I to 121 Sv in State II. This change occurs because of a change in the difference in bottom pressure between the two sides of the model's Drake Passage as a result of a stronger NADWF in State II. Previous studies (e.g., Pierce *et al.* 1995; Cai and Baines 1996) have found that the pressure difference across the Drake Passage is strongly influenced by the northern overturning circulation via the model NADWF outflow.

4. DISCUSSION AND CONCLUSIONS

An important question is whether the climate would fully return to that of the present day if the atmospheric CO_2 level, after doubling, were to return to its present-day level. Although an ultimate answer must be obtained from a realistic coupled model, the present study provides some insights. In view of the mechanistic nature of our study, several caveats are in order.

Firstly, the present study does not address the effects of changes in fresh-water fluxes. Coupled models have shown that changes in meridional temperature- gradients in response to increasing CO_2 are accompanied by changes in atmosphere–ocean fresh-water fluxes via an enhancement of the hydrological cycle with increased high-latitude fresh-water input from the atmosphere to the ocean. There are no obvious ways in which these processes may be included in our simple model. Previous studies (e.g., Stocker and Wright 1991; Rahmstorf 1995a) have demonstrated that, in response to gradual changes in high-latitude fresh-water fluxes, the thermohaline circulation behaves in a manner similar to that in our study. We note that as CO_2 increases, the associated changes in SST and in fresh-water fluxes both act to enhance the surface buoyancy-fluxes at high latitudes. Thus in terms of contributions to surface buoyancy, changes in SST and fresh-water flux as CO_2 increases do not offset each other. Consequently, the qualitative features of the responses discussed in section 3 may still appear even if the enhancement of hydrological cycle is included.

Secondly, the seasonal cycle, the bathymetry and bottom topography are not included. Their effects are not clear. In the model of Rahmstorf (1995a), which has a realistic bottom topography, similar features of response appear, indicating that the inclusion of a bottom topography may not significantly alter them.

Finally, in fully coupled models, the thermohaline circulation appears to be very stable, and recovers after an external forcing is removed (Manabe and Stouffer 1993, 1994). The present study indicates that, within the thermally dominant regime, the convection patterns and distribution of SSTs may be different, although the difference in the maximum overturning may be small. It is not clear in these coupled models how the convection patterns and SSTs of the recovered state differ from those in the state before the forcing.

To conclude, we have shown that there is a lag between a change in thermal forcing and the response of the thermohaline circulation, and that, under identical forcing conditions, many states of quasi-equilibrium may be generated within the thermally driven regime. We have also demonstrated that changes in atmospheric thermal conditions can push the system into an oscillatory regime. These behaviour patterns suggest that climate change in the coupled system may not be fully reversible. In particular, the oceanic climate may not regain its former state; the maximum oceanic overturning circulation associated with different states of quasi-equilibrium may be similar, but the strength and location of oceanic convection may differ significantly. So may SSTs.

REFERENCES

Bond, G., Broecker, W., Johnsen, S., McManus, J., Labeyrie, L., Jouzel, J. and Bonani, G.   1993   Correlations between climate records from North Atlantic sediments and Greenland ice. *Nature*, **365**, 143–147

Broecker, W. S., Peteet, D. M. and Rind, D.   1985   Does the ocean–atmosphere system have more than one stable mode of operation? *Nature*, **315**, 21–26

Bryan, K.   1969   A numerical method for the study of the circulation of the world ocean. *J. Comput. Phys.*, f4, 347–376

        1984   Accelerating the convergence to equilibrium of ocean–climate models. *J. Phys. Oceanogr.*, **14**, 666–673

Bryan, F.   1986   High-latitude salinity effects and interhemispheric thermohaline circulation. *Nature*, **323**, 301–304

Bryan, F.   1987   Parameter sensitivity of primitive equation ocean general circulation models. *J. Phys. Oceanogr.*, **17**, 970–985

Bryan, K., Manabe, S. and Spelman, M. J.   1988   Interhemispheric asymmetry in the transient response of a coupled ocean–atmosphere model to a CO_2 forcing. *J. Phys. Oceanogr.*, **18**, 851–867

Cai, W.   1996a   The stability of NADWF under mixed boundary conditions with an improved diagnosed fresh-water flux field. *J. Phys. Oceanogr.*, **26**, 1081–1087

    1996b   Generation of thermal oscillations in an ocean model. *Q. J. R. Meteorol. Soc.*, **122**, 1721–1738

Cai, W. and Baines, P. G.   1996   Interactions between thermohaline and wind-driven circulations and their relevance to the dynamics of the Antarctic Circumpolar Current, in a coarse resolution global OGM. *J. Geophys. Res.*, **101**, 14073–14093

Cai, W. and Chu, P.   1996   Ocean climate drift and interdecadal oscillation due to a change thermal dumping. *J. Climate.*, **9**, 2821–2833

    1998   A thermal oscillation under a restorative forcing. *Q. J. R. Meteorol. Soc.*, **124**, 793–809

Cai, W. and Gordon, H. B.   1998   Responses of the CSIRO climate model to two different rates of CO_2 increase. *Climate Dynamics*, **14**, 503–516

Cai, W., Greatbatch, R. J. and Zhang, S.   1995   Interdecadal variability in an ocean model driven by a small, zonal redistribution of the surface buoyancy flux. *J. Phys. Oceanogr.*, **25**, 1998–2010

Cai, W., Syktus, J., Gordon, G. H. and O'Farrell, S.   1997   Response of a global coupled ocean–atmosphere–sea-ice climate model to an imposed North Atlantic high-latitude freshening. *J. Climate*, **10**, 929–948

Cubasch, U., Hasselmann, K., Rock, H., Maier-Reimer, E., Mikolajewicz, U., Santer, B. D. and Sausen, R.   1992   Time-dependent greenhouse warming computation with a coupled ocean–atmosphere model. *Climate Dynamics*, **8**, 55–69

Duplessy, J. C., Shackleton, N. J., Fairbanks, R. G., Labeyrie, L., Oppo, D. and Kallel, N.   1988   Deep-water source variations during the last climate cycle and their impact on the global deep-water circulation. *Paleoceanography*, **3**, 343–360

Gordon, H. B. and O'Farrell, S.   1997   Transient climate change in the CSIRO coupled model with sea-ice dynamics. *Mon. Weather Rev.*, **125**, 875–907

Greatbatch, R. J. and Peterson, K. A.   1996   Interdecadal variability and oceanic thermohaline adjustment. *J. Geophys. Res.*, **101**, 20467–20482

Griffies, S. M. and Tziperman, E.   1995   A linear thermohaline oscillator driven by stochastic atmospheric forcing. *J. Climate*, **8**, 2440–2453

Huang, R. X. and Chou, L.   1994   Parameter sensitivity study of the saline circulation. *Climate Dynamics*, **9**, 391–409

Huang, R. X., Luyten, J. R. and Stommel, H. M   1992   Multiple equilibrium states in combined thermal and saline circulation. *J. Phys. Oceanogr.*, **22**, 231–246

Lenderink, G. and Haarsma, R. J.   1994   Variability and multiple equilibria of the thermo-haline circulation, associated with deep-water formation. *J. Phys. Oceanogr.*, **24**, 1480–1493

    1996   Rapid convective transitions in the presence of sea-ice. *J. Phys. Oceanogr.*, **26**, 1448–1467

Maier-Reimer, E. and Mikolajewicz, U.   1989   Experiments with an OGM on the cause of the Younger Dryas. *Oceanography*, UNAM Press, 87–100

Manabe, S. and Stouffer, R. J.   1988   Two stable equilibria of a coupled ocean–atmosphere model. *J. Climate*, **1**, 841–866

    1993   Century-scale effects of increased atmospheric CO_2 on the ocean–atmosphere system. *Nature*, **364**, 215–218

    1994   Multiple-century response of a coupled ocean–atmosphere model to an increase in atmospheric carbon dioxide. *J. Climate*, **7**, 5–23

    1995   Simulation of abrupt climate-change induced by fresh-water input to the North Atlantic Ocean. *Nature*, **378**, 165–167

Manabe, S., Bryan, K. and Spelman, M. J.   1990   Transient response of a global ocean–atmosphere model to a doubling of atmospheric carbon dioxide. *J. Phys. Oceanogr.*, **20**, 722–749

Manabe, S., Stouffer, R. J., Spelman, M. J. and Bryan, K.   1991   Transient response of a coupled ocean–atmosphere model to gradual changes of atmospheric CO_2. Part I: Annual mean response. *J. Climate*, **4**, 785–818

Marotzke, J.   1994   'Ocean models in climate problem.' Pp. 79–109 in *Ocean process in climate dynamics: Global and Mediterranean examples.* Eds P. Malanatte-Rizzoli and A. R. Robinson, Kluwer Academic Publishers

Murphy, J. M. and Mitchell, J. F. B.   1995   Transient response of the Hadley Centre coupled ocean–atmosphere model to increasing carbon dioxide. Part II: Spatial and temporal structure of response. *J. Climate,* **8,** 57–80

Oppo, D. and Fairbanks, R. G.   1990   Atlantic ocean thermohaline circulation for the last 150 000 years: Relationship to climate and atmospheric CO_2. *Paleoceanography,* **5,** 277–288

Pacanowski, R. C., Dixon, K. W. and Rosati, A.   1991   GFDL 'Modular Ocean Model Users Guide Version 1.0.' GFDL Ocean Group Tech. Rep. No. 2, GFDL/Princeton University, Princeton, N.J., USA

Pierce, D. W., Barnett, T. P. and Mikolajewicz, U.   1995   Competing roles of heat and fresh-water flux in forcing thermohaline oscillations. *J. Phys. Oceanogr.,* **25,** 2046–2064

Rahmstorf, S.   1995a   Bifurcation of the Atlantic thermohaline circulation in response to changes in the hydrological cycle. *Nature,* **378,** 145–149

                                      1995b   Multiple convection patterns and thermohaline flow in an idealized OGCM. *J. Climate,* **8,** 3028–3039

Rahmstorf, S. and Willebrand, J.   1995   The role of temperature feedback in stabilizing the thermohaline circulation. *I. Phys. Oceanogr.,* **25,** 787–805

Raymo, M. E, Ruddiman, W. F., Shackleton, N. J. and Oppo, D. W.   1990   Evolution of Atlantic–Pacific d13O gradients over the last 2.5 m.y. *Earth Planet. Sci. Lett.,* **97,** 353–368

Schopf, P. S.   1983   On equatorial waves and El Niño. II: Effects of air–sea thermal coupling. *J. Phys. Oceanogr.,* **13,** 1878–1893

Stocker, T. F. and Wright, D. G.   1991   Rapid transitions of the ocean's deep circulation induced by changes in surface water fluxes. *Nature,* **351,** 729–732

Stommel, H.   1961   Thermohaline convection with two stable regimes of flow. *Tellus,* **13,** 224–230

Stouffer, R. J., Manabe, S. and Bryan, K.   1989   Interhemispheric asymmetry in climate response to a gradual increase of atmospheric CO_2. *Nature,* **89,** 571–586

Tziperman, E., Toggweiler, J. R., Feliks, Y. and Bryan, K.   1994   Instability of the thermohaline circulation with respect to mixed boundary conditions: is it really a problem for realistic models. *J. Phys. Oceanogr.,* **24,** 217–232

Weaver, A. J. and Hughes, T. M. C.   1994   Rapid interglacial climate fluctuations driven by North Atlantic ocean circulation. *Nature,* **367,** 447–450

Weaver, A. J. and Sarachik, E. S.   1991a   The role of mixed boundary conditions in numerical models of the ocean's climate. *J. Phys. Oceanogr.,* **21,** 1470–1493

                                      1991b   Evidence for decadal variability in an ocean general circulation model: an advective mechanism. *Atmosphere–Ocean,* **29,** 197–231

Winton, M.   1996   On the role of horizontal boundaries in parameter sensitivity and decadal-scale variability of coarse-resolution ocean general circulation models. *J. Phys. Oceanogr.,* **26,** 289–304

                                      1997   The damping effect of bottom topography on internal decadal-scale oscillations of the thermohaline circulation. *J. Phys. Oceanogr.,* **27,** 203–208